

FINITE ELEMENT MODELING OF FLEXURE/SHEAR BEHAVIOR OF R/C SLABS

M. S. A. Abbasi*, M. H. Baluch, A. K. Azad
and H. H. Abdel Rahman

*Department of Civil Engineering
King Fahd University of Petroleum & Minerals
Dhahran, Saudi Arabia*

الخلاصة :

تقدم ورقة العمل هذا أشكال الفشل المختلفة للبلاطات الخرسانية المسلحة والتي حدثت إما بسبب تشوهات شد في الخرسانة أو بسبب خضوعٍ لدنٍ يؤدي إلى تمشم الخرسانة . ويمكن تصنيف الأشكال الشائعة لانتهيار هذه البلاطات على أساس درجة كل من مركبات هذا الفشل . ويساعد مثل هذا التصنيف على الفصل بين الفشل للبلاطات الخرسانية المسلحة الناتج عن الانحناء المصحوب بالقص أو الناتج عن قص الثقب أو القص الخالص . ولقد تمَّ إيضاح تأثير حديد تسليح الشدِّ الرئيسي على التغير في أشكال الفشل المختلفة لبلاطة خرسانية مسلحة ومعرضة لحمل سطح موزع مقياسه بالنسبة للبلاطة يعطى نسبة مماثلة لنسبة أثر إطار سيارة إلى بلاطة جسر وذلك باستخدام نموذج غير خطي للعناصر المحددة . تعرض هذه الدراسة بوضوح مقتضيات هذا النموذج لمنع أشكال الانتهيار المحتمل لأرضيات الجسور المكونة من بلاطة كمرية أو كمرية صندوقية .

*Address for correspondence:
KFUPM Box No. 938
King Fahd University of Petroleum & Minerals
Dhahran 31261
Saudi Arabia

ABSTRACT

This paper delineates the various failure modes of a RC slab in terms of damage dominated either by tension cracking in concrete or plastic yielding leading to concrete crushing. Commonly observed failure modes of such slabs are classified according to level of each damage component. Such a classification helps separate the flexure–shear failure mode of RC slabs from the true punching or shear mode of collapse. The influence of main tensile reinforcement on the metamorphosis in failure modes is highlighted by use of a non-linear finite element model, using patch loads where size bear a similar ratio to the size of the slab as the ratio of the print of a wheel to the size of a deck slab. The implications of this model to preclude the most probable mode of failure in girder–slab or box-girder deck systems are highlighted.

FINITE ELEMENT MODELING OF FLEXURE/SHEAR BEHAVIOR OF R/C SLABS

1. INTRODUCTION

Several papers addressing various aspects of flexural and shear failure of reinforced concrete slabs have appeared in a steady stream over the past twenty five years or so, but there appears to be a lack of consensus on the role of the various characteristic parameters influencing failure. This is reflected in the conservative approach adopted by the design codes, with the ACI Code not reflecting the beneficial effect of main reinforcement on punching resistance, and both BS 8110 and ACI neglecting any contribution of edge restraint to punching capacity.

The influence of several factors on the punching and flexural capacities of reinforced concrete slabs has been considered by various authors—with effect of edge restraint taking precedence over most. Taylor and Hayes [1] published some test data on the effect of edge restraint on punching shear in RC slabs. The results reflected an interesting phenomenon that the beneficial effect of edge restraint on the failure load, identified as punching, appeared to taper off as the main reinforcement percentage was increased. Other authors subsequently cited similar observations [2–4], but the interaction of several variables in a complex manner continued to preclude the development of a universal approach for the design of restrained slabs. An interesting series of papers by Regan and his coworkers [5–7] has encompassed a wide ranging study on punching of RC slabs, discussing influence of several parameters including arrangement of flexural reinforcement, slab depth, concrete strength, ratio of reinforcement, boundary restraint, and size of the loaded area. A considerable amount of experimental data has been presented, and a model hypothesized to predict punching resistance of slabs, using an approach which may be considered to be an extension of the Kinnunun–Nylander model [8].

There exists voluminous literature addressing the flexural response of slabs, especially pertaining to enhancement of slab strength due to compressive membrane action [2, 9–11]. Based on the favorable influence of membrane forces on the strength of slabs, the Ontario Bridge Design Code [12] introduced an empirical design method using 0.3% isotropic steel at both top and bottom faces of the slab.

In addition to the several predictor models and results of experimental investigations published, elegant solutions based on plasticity models for punching shear and flexural response of slabs also exist [13–15], showing that the subject of flexural/punching response of RC slabs continues to attract considerable attention.

In the work presented thus far, the one serious limitation appears to be the lack of definition of what constitutes a true punching failure, and as a consequence, the delineation or demarcation of the zone that lies between pure flexure and pure punch or the zone of flexure–shear interactive failure. The one single observation that has led most experimentalists to believe that the phenomenon being observed in the laboratory, for the case of patch loads whose size bear a similar ratio to the size of the slab as the ratio of the print of a wheel to the size of a deck slab, is one of punching is the (inevitable) occurrence of the sudden displacement of the shear cone relative to the rest of the slab under application of load, with no indication of development of full yield-line mechanism, *i.e.* yielding is localized to the small region of loaded area. As will be shown, this mode of failure is peculiar not only to pure shear or punching failure, but also to a combined flexural–shear failure.

2. MATERIAL MODELING

In order to observe the influence of area of tensile reinforcement (and other relevant parameters) on the flexure/shear response of reinforced concrete slabs, a non-linear finite element formulation was adopted, using non-linear components of material response along lines similar to the one adopted by Owen and Figueiras [16]. The non-linear components considered in this model include:

1. Plastic flow of concrete according to a prescribed yield criterion in terms of stress invariants
2. Concrete cracking, including tension stiffening
3. Shear degradation
4. Crushing of concrete according to a yield criterion in terms of strain invariants
5. Elasto–Plastic behavior of steel reinforcement.

2.1. Stress Yield Criterion

Mohr–Coulomb yield criterion, which has been used successfully for shear critical reinforced concrete beams [17], was used and expressed in terms of stress invariants I_1 , J_2 , and J_3 as

$$F(\sigma_{ij}) = \frac{2}{(1 - \sin \phi)} \left[\frac{I_1}{3} \sin \phi + \sqrt{J_2} \left(\cos \theta - \frac{1}{\sqrt{3}} \sin \theta \sin \phi \right) \right] - f'_c = 0 \quad (1)$$

where $\sin 3\theta = -3\sqrt{3}J_3/(2(J_2)^{3/2})$.

In addition, in order to construct the stress–strain relationship in the plastic range, assuming normality of the plasticity deformation rate vector to the yield surface in the form

$$d\epsilon_{ij}^p = d\lambda \frac{\partial F(\sigma)}{\partial \sigma_{ij}} \quad (2)$$

the elasto-plastic constitutive matrix D_{ep} may be shown to be [18]

$$[D_{ep}] = [D] - \frac{[D][a][a]^T[D]}{H' + [a]^T[D][a]} \quad (3)$$

where $[D]$ is a (5×5) elastic constitutive matrix, $[a]$ is the (5×1) flow vector with

$$[a]^T = \frac{\partial F}{\partial \{\sigma\}} = \frac{\partial F}{\partial I_1} \frac{\partial I_1}{\partial \{\sigma\}} + \frac{\partial F}{\partial \sqrt{J_2}} \frac{\partial \sqrt{J_2}}{\partial \{\sigma\}} + \frac{\partial F}{\partial \theta} \frac{\partial \theta}{\partial \{\sigma\}} \quad (4)$$

where $\{\sigma\}^T = \{\sigma_x, \sigma_y, \tau_{xy}, \tau_{xz}, \tau_{yz}\}$. H' is the hardening parameter as obtained from uniaxial compression test data.

Eliminating θ in terms of J_2 and J_3 , Equation (4) may be recast in the form

$$[a] = C_1[a_1] + C_2[a_2] + C_3[a_3] \quad (5)$$

where

$$[a_1]^T = \frac{\partial I_1}{\partial \{\sigma\}} = \{1, 1, 0, 0, 0\} \quad (6)$$

$$[a_2]^T = \frac{\partial \sqrt{J_2}}{\partial \{\sigma\}} = \frac{1}{2\sqrt{J_2}} \{\sigma_x, \sigma_y, 2\tau_{xy}, 2\tau_{xz}, 2\tau_{yz}\} \quad (7)$$

$$[a_3]^T = \frac{\partial J_3}{\partial \{\sigma\}} = \left[\left(\sigma_y' \sigma_z' - \tau_{yz}^2 + \frac{J_2}{3} \right), \left(\sigma_x' \sigma_z' - \tau_{xz}^2 + \frac{J_2}{3} \right), 2(\tau_{yz} \tau_{xz} - \sigma_z' \tau_{xy}), 2(\tau_{xy} \tau_{yz} - \sigma_y' \tau_{xz}), 2(\tau_{xz} \tau_{xy} - \sigma_x' \tau_{yz}) \right] \quad (8)$$

and

$$C_1 = \frac{\partial F}{\partial I_1} = \frac{M}{3} \sin \phi \quad (9)$$

$$C_2 = \frac{\partial F}{\partial \sqrt{J_2}} - \frac{\tan 3\theta}{\sqrt{J_2}} \frac{\partial F}{\partial \theta} = M \cos \theta [(1 + \tan \theta \tan 3\theta) + \sin \phi (\tan 3\theta - \tan \theta) / \sqrt{3}] \quad (10)$$

$$C_3 = M(\sqrt{3} \sin \theta + \cos \theta \sin \phi) / (2J_2 \cos 3\theta) \quad (11)$$

where $M = 2/(1 - \sin \phi)$.

The casting of the Mohr–Coulomb criterion in the form of Equation (1) renders convenient the adaptability of the formulation to either perfectly plastic models or to strain-hardening models, where f'_c can be replaced by the effective stress σ_o .

Hardening for concrete was incorporated by extrapolating from results of uniaxial stress–strain relationship given by the “Madrid Parabola” [16]

$$\sigma = E_o \epsilon - \frac{1}{2} \frac{E_o}{\epsilon_o} \epsilon^2 \quad (12)$$

where E_o is the initial elasticity modulus of concrete, ϵ_o is the strain at peak stress $f'_c (= 2f'_c/E_o)$ and (σ, ϵ) represent the stress and total strain in the uniaxial test. Using the concept of effective stress and effective plastic strain, Equation (12) was used to determine the effective stress level $\sigma = \sigma_o$ and the hardness parameter $H' = d\sigma/d\epsilon_p$, where ϵ_p is the plastic strain component of the total strain, for the current loading surface position.

Other components contributing to non-linear behavior of the RC slab including tension stiffening and elasto-plastic behavior of steel reinforcement were taken as described in detail in [16], with the concrete crushing criterion in terms of total strains expressed as (Von Mises strain criterion)

$$[\varepsilon_x^2 + \varepsilon_y^2 - \varepsilon_x \varepsilon_y + 0.75(\gamma_{xy}^2 + \gamma_{yz}^2 + \gamma_{zx}^2)]^{1/2} = \varepsilon_u \quad (13)$$

where ε_u is an ultimate total strain extrapolated from uniaxial test results and taken as 0.0035. The material is assumed to lose all its characteristics of strength and rigidity when ε_u at a specific (Gauss) point reaches 0.0035.

3. FINITE ELEMENT MODEL

A computer code 'FATIMA' has been developed for reinforced concrete plates and shells using the nine noded heterosis element derived from the degeneration of a three dimensional element, following the format outlined in [16]. Five degrees of freedom are specified at each nodal point, corresponding to its three displacements and two rotations of the normal at that node. This approach reduces to Mindlin plate hypothesis when applied to plate bending problems wherein transverse shear deformation is accounted. A layered model is used in order to observe progressive damage through the thickness. Stresses, strains and change in the characteristics of material are monitored at Gauss integration points in each layer. Any material represented at a Gauss point may remain elastic, yield, crush or crack. It is possible that the material may crack in one direction whilst yielding at the same time. Cracking is allowed to occur in one or two directions in planes normal to the plane of layer *i.e.*, the cracking is assumed to be initiated in one and/or two directions when one and/or two principal inplane stresses reach the tensile strength of concrete. Cracks are allowed to close and reopen in one or two directions upon unloading and reloading of the slab. However, the yielding and crushing of concrete is governed under general state of stress.

Shear failure is attributed to the out of plane shear degradation due to increased circumferential cracking. Shear failure is identified by tracing locus of the damage zones through the thickness.

For the slabs analyzed in this work as a test example, the depth is discretized into eight layers and two steel layers. As far as the mesh is concerned, further refinement did not improve accuracy of results in terms of ultimate load and cracking pattern. On the other hand, results are quite sensitive to the number of concrete layers. Selective integration scheme is employed using normal 3×3 integration rule for bending and membrane energy terms and 2×2 integration rule for shear terms.

An incremental and iterative modified Newton–Raphson scheme is employed for the nonlinear analysis and the tangential stiffness matrix is recalculated for the second iteration of each load increment. Convergence criterion in terms of displacements and rotations is used separately. For convergence the maximum number of iterations was set to twenty for a tolerance of one percent.

4. RESULTS AND DISCUSSION

As a test example, the slabs used by Taylor and Hayes [1] in their experimental work were adopted for simulation. The slabs were $890 \times 890 \times 76$ mm ($35 \times 35 \times 3$ in) and experimental loads were presented for total steel percentages of $\rho = 1.57$ and $\rho = 3.14$. The slabs were tested as pairs—one unrestrained and simply supported, with the other of the pair being restrained.

The slab geometry and finite element discretization is shown in Figure 1, with the slab being subdivided into eight concrete layers. Steel of equal amount was placed in two orthogonal layers.

The material properties used in the numerical analysis were: $f'_c = 29 \text{ N mm}^{-2}$; $E_c = 28\,460.5 \text{ N mm}^{-2}$; $f_t = 2.9 \text{ N mm}^{-2}$; $\varepsilon_u = 0.0035$; $\varepsilon_c = 0.005$; $\varepsilon_m = 0.002$; $\alpha = 0.7$; $f_y = 375.8 \text{ N mm}^{-2}$; $E_s = 200\,000 \text{ N mm}^{-2}$; $E'_s = 2\,800 \text{ N mm}^{-2}$.

In order to highlight flexure–shear interactive modes of failure, the ratio of characteristic size of patch load to slab must be similar to that of the wheel print to the deck slab. Results are shown for two cases, one with a patch load of size $50.8 \text{ mm} \times 50.8 \text{ mm}$ and the other for a patch load of size $101.6 \text{ mm} \times 101.6 \text{ mm}$.

Shown in Figure 2 is the spectrum of failure loads as obtained for values of total reinforcement in the two directions, ρ , ranging from 0.3% to 6.28%, for a patch load of size $50.8 \text{ mm} \times 50.8 \text{ mm}$. Also superimposed in Figure 2 is the locus of ultimate capacity as obtained from ACI and BS 8110 and experimental values as reported in [1].

The behavior may be demarcated into three zones as given by

- $0 \leq \rho \leq \rho_I$: Flexure Mode Dominated Failure (Zone I)
- $\rho_I \leq \rho \leq \rho_{II}$: Combined Flexure–Shear Mode Failure (Zone II)
- $\rho > \rho_{II}$: Shear Mode Failure (Zone III).

For $\rho < \rho_I$ ($= 0.75\%$), the yield line analysis serves as a lower bound estimate to the capacity of the slab.

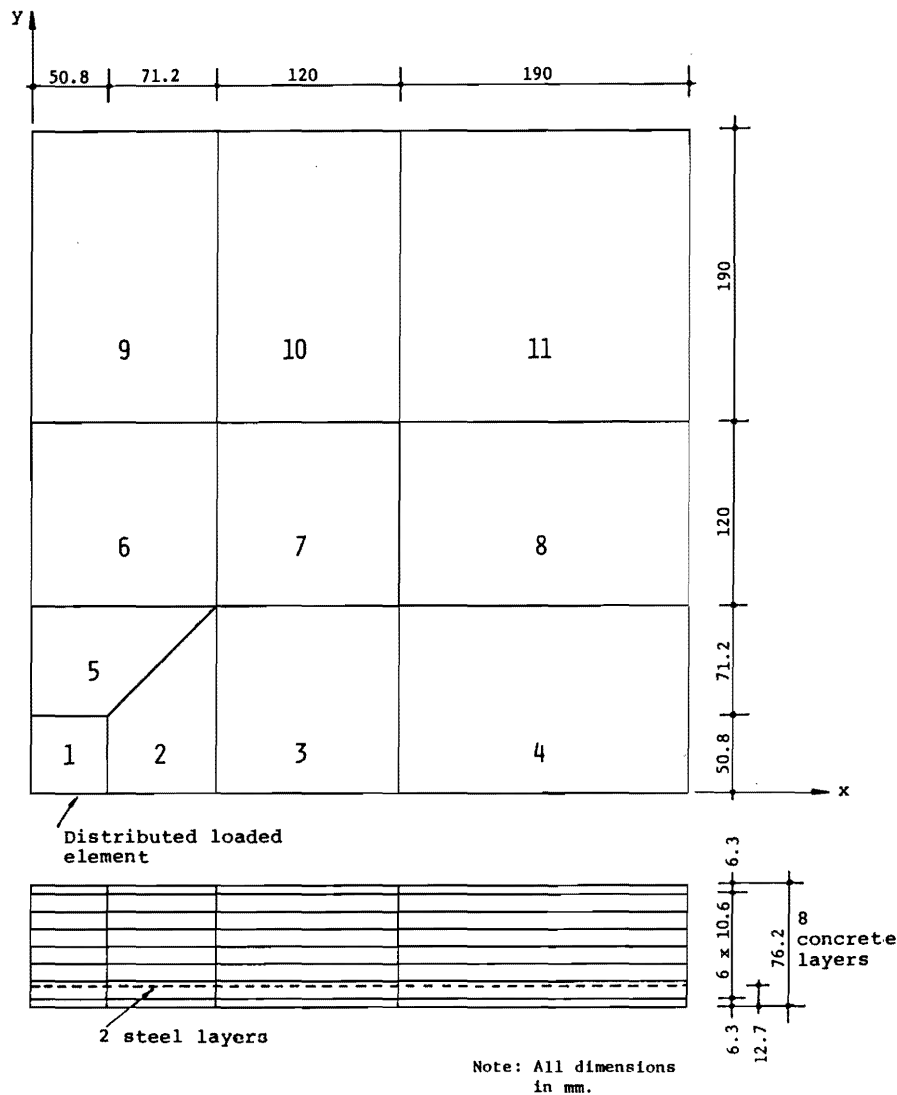


Figure 1. Finite Element Discretization for Slab.

The failure loads as obtained from the model in this zone are somewhat larger than the yield line loads—this is attributed to the load carrying capacity of plain concrete (due to its tensile strength) which is neglected in yield line analysis. Failure in this region ($\rho = 0.6\%$) was marked by deep intrusion of tension cracks, yielding of tension reinforcement along diagonal lines and a measure of ductility.

In Zone II ($0.75 \leq \rho \leq 3.5\%$), the failure load continues to be influenced by area of steel reinforcement, albeit at a decreasing rate. Here, the yield line analysis does not reflect the true failure mode of the slab, as ultimate conditions are marked by decreasing ductility and lowered level of yielding of steel reinforcement. Tension cracking damage intrusion was

arrested at lower depths by increased steel percentage—leading to increase in ultimate load. This zone reflects characteristics of a combined flexure–shear failure mode.

In Zone III defined by $\rho > 3.5\%$, the failure load as predicted by the model remains by large unaffected by increases in steel percentage and becomes asymptotic to what may be construed to be the true punching capacity. Tension cracking damage, prior to sudden collapse, is minimal. Failure is characterized by gross brittle response, with little or no yielding of reinforcement.

Figure 3 shows the failure load–total reinforcement variation for a patch load of size $101.6\text{mm} \times 101.6\text{mm}$.

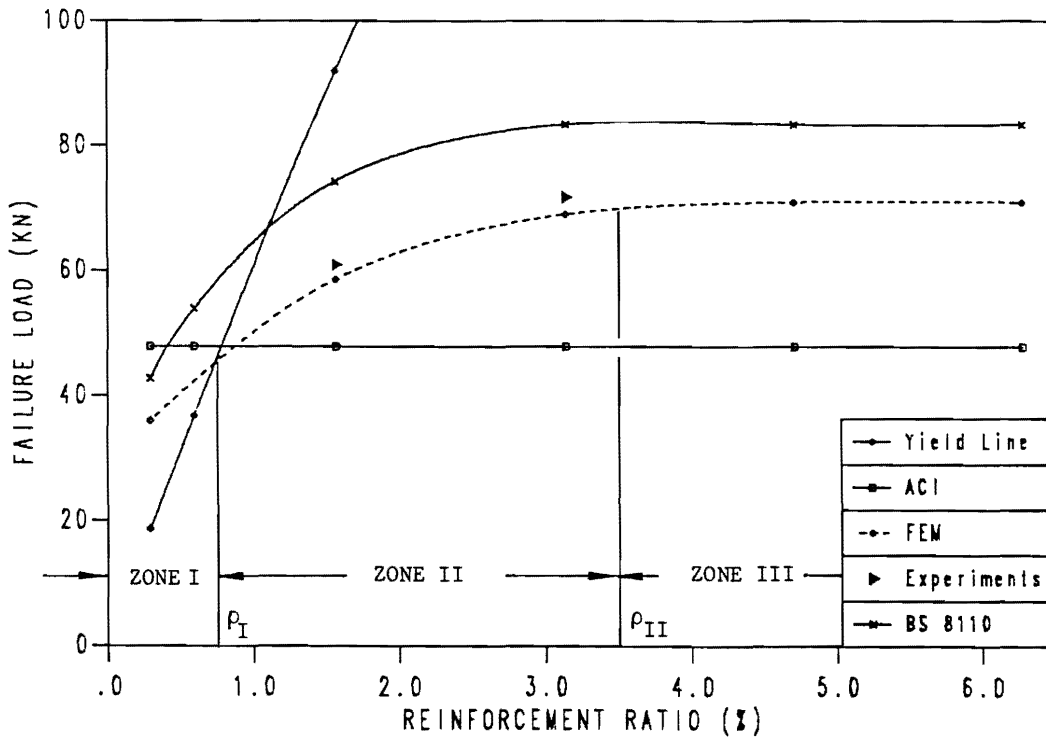


Figure 2. Failure Load vs Total Reinforcement Ratio ρ (Patch size 50.8 mm \times 50.8 mm).

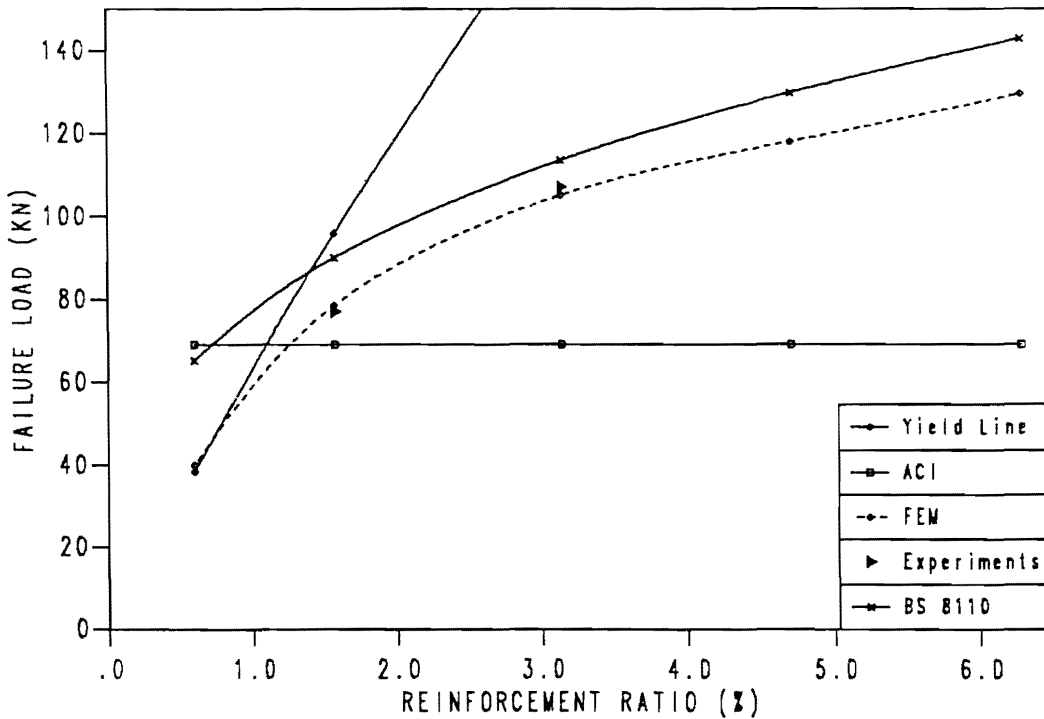


Figure 3. Failure Load vs Total Reinforcement Ratio ρ (Patch size 101.6 mm \times 101.6 mm).

One notes that the zones demarcating flexure and shear modes have shifted. The collapse load continues to be influenced by amount of steel (although at an increasingly lower rate) for ρ as high as 6.28%, which corresponds to $\rho = 3.14\%$ in each direction for isotropically reinforced slabs. For this case, the true punching capacity was taken to be the collapse load corresponding to total $\rho = 6.28\%$, although the asymptotic value will be reached at a slightly higher value of ρ .

In all cases considered, it was interesting to note the formation of radial tensile cracks first, followed subsequently by circumferential tensile cracking. Figure 4 shows the profile of two way cracking for the slab reinforced with $\rho = 6.28\%$ at a load level $P = 0.76 P_u$. It is this two way cracking, accompanied by shear degradation in cracked zones, that forms the basis of the interactive shear-flexure failure modes.

4.1. Failure Modes of a Reinforced Concrete Slab

Proceeding on a basis that the various failure modes of a reinforced concrete slab subjected to a patch load over a small central zone encompass a spectrum ranging from pure flexural failure (yield line solution) to that of pure shear failure (punching capacity), the primary variable influencing such a transition is the area of main or tensile reinforcement in the slab. This hypothesis may be supported with the following sequence of damage occurring phenomenon in slabs:

1. At very low levels of main reinforcement (weakly reinforced slabs), initial damage to the slab occurs in the form of tension cracking in the radial direction and such cracks propagate upwards with a low arrest factor.

With increasing load, cracks are also formed in the circumferential direction with accompanying

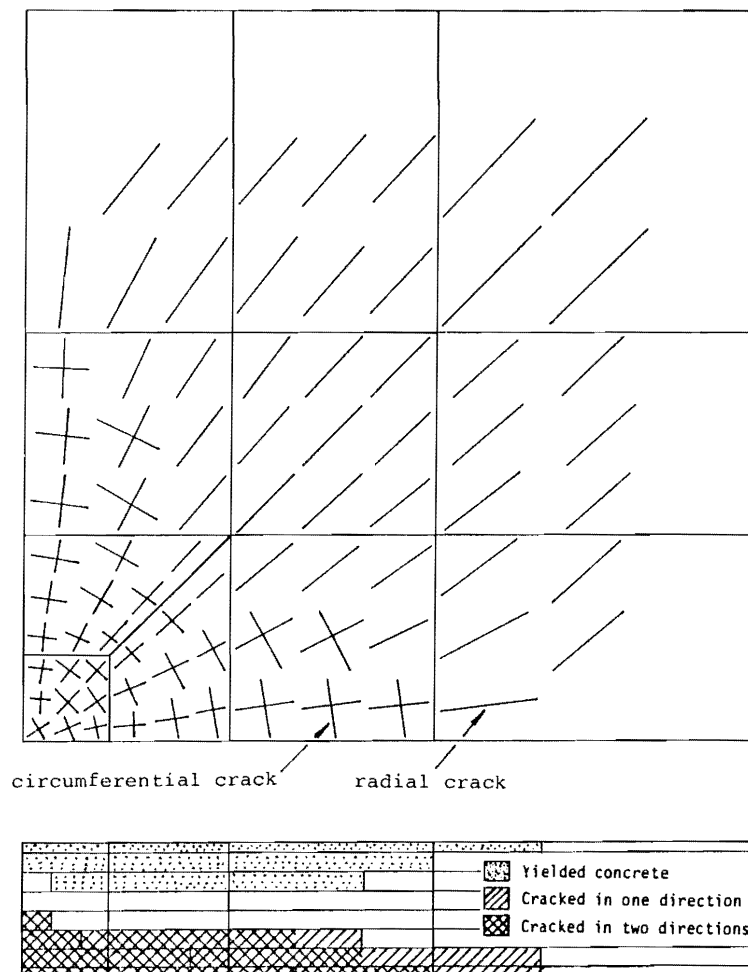


Figure 4. Cracking Profile at $P/P_u = 0.76$ ($\rho = 6.28\%$).

degradation in shear transfer mechanism. The damage zone at incipient failure is dominated by two way tension cracking extending to almost the full depth, leading to separation along a significant portion of the potential punching shear collapse surface. By virtue of this separation, failure occurs at a load significantly lower than the true punching or shear capacity of the panel. Results for the slab subjected to a central patch load of size 101.6 mm × 101.6 mm and reinforced with $\rho = 0.6\%$ are representative of this behavior, with deep intrusions of tension cracking damage (Figure 5a) prior to eventual collapse. The collapse load recorded was only 31% of the full punching shear capacity of the panel, with the latter being defined to be attained for the case where separation along potential shear collapse surface is minimized, *i.e.* a highly reinforced slab.

Failure of weakly reinforced slabs is typified by a measure of ductility (due to plastic flow of reinforcement) and wide cracks—and can be termed a soft failure since energy is released gradually. The failure load of such slabs would be close to that given by a yield line analysis.

- At medium levels of main reinforcement, initial damage to the slab again occurs in the form of tension cracking in the radial direction, but the crack arrest factor is higher due to increased reinforcement. As in the previous case, circumferential cracks are initiated at higher loads subsequently. However, as seen in the results for the case of a slab representative of this case (reinforced with $\rho = 3.14\%$ (Figure 5b)), the damage zone prior to impending failure is not as preponderantly two way cracking as the case of the weakly reinforced slab. Thus a greater portion of the potential shear collapse surface remains in contact and undegraded in shear transfer. The intact segment of the potential collapse surface is subjected to high shear and compressive stresses, leading to plastic flow.

The plastic flow leads to increased strains in the concrete, which then begins to crush under an appropriate crushing criterion (in the neighborhood of the load). The final event in the collapse mechanism is a sudden displacement of the shear cone relative to the rest of the slab—and it is this phenomenon which has been misconstrued to represent a punching or shear failure. This in reality is a combined flexure–shear failure, with significant damage components from both modes.

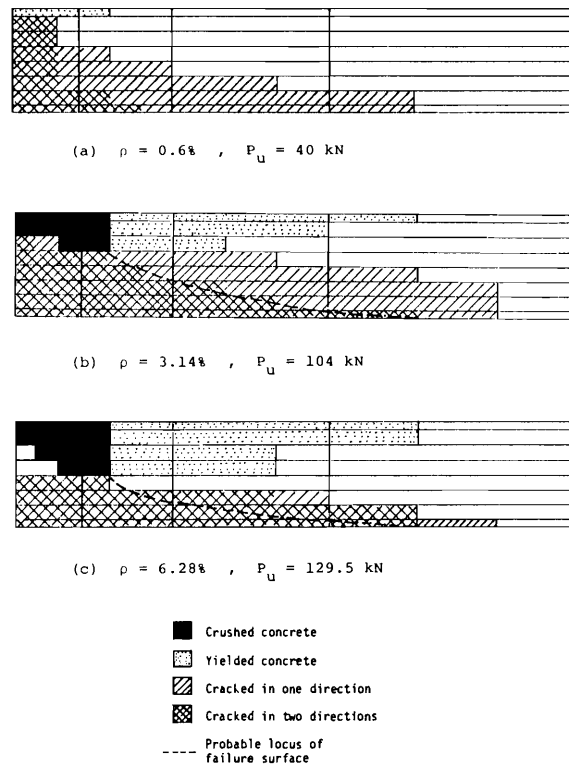


Figure 5. Influence of Total Reinforcement Ratio ρ on Damage Zone at Ultimate Load P_u .

Failure of such slabs is typified by decreased ductility—since there is decreased yielding or flow of reinforcement, although accompanied by greater plastic flow of concrete. However, ultimate strains in flowing concrete are significantly lower than those in yielding steel. The failure can be termed as semi-soft, because the displacement of the shear cone as the ultimate event is accompanied by a sudden release of energy. The failure load of such slabs cannot be predicted by either yield line analysis nor by a pure shear or punch analysis.

- At high levels of main reinforcement, initial damage is essentially restricted to minimal tension cracking, with cracks being arrested prior to any significant growth. The potential collapse surface is mostly intact by virtue of compressive stresses acting across it. Further damage to the slab can occur only subsequent to plastic flow of the large, undamaged concrete region culminating in crushing of concrete. The final event in this collapse mode is also a sudden displacement of the shear cone relative to the rest of the slab—

but is different from failure as in (2) in that it is preceded by minimal tension cracking damage prior to punching action.

Damage zone for panel reinforced with $\rho = 6.28\%$ (Figure 5c) is construed to be representative of this mode of behavior, and the collapse load of $P_u = 129.5$ kN is taken as a measure of the true punching capacity of the 76.2 mm (3 in) thick reinforced concrete slab, subject to a load distributed on a central patch of size 101.6 mm \times 101.6 mm (4 in \times 4 in).

Failure of such slabs is explosive and marked by minimum ductility—since although concrete is in a state of plastic flow, the tension reinforcement is mostly in the elastic region. Thus the degree of plasticity of a composite structure such as a RC slab must be viewed with reference to degree of flow of each material component. This reasoning also explains how punching models based on plasticity formulation [13, 15] can predict failure loads of a seemingly overall brittle phenomenon—queried as an apparent dichotomy by certain researchers. The failure load of such slabs can be approximately predicted by punching shear plasticity models [19], in which the basic assumption is an intact potential collapse surface prior to failure and which is realized only in the presence of high main reinforcement. Such failures represent a pure shear or a true punch failure of RC slabs.

4.1.1. Influence of Support Restraint

The effect of support restraint on enhancement of collapse load of the panel was modeled by laterally restraining the four edges of the slab ($u = v = 0$), and an increase of 8.2% in the collapse load was noted for the slab with total $\rho = 3.14\%$. Figure 6 shows the damage zones at incipient failure, and the depth of the crushed zone is more of the order of an unrestrained slab of higher ρ (Figure 5c) rather than that of its own counterpart unrestrained case (Figure 5b). Thus the overall effect of support restraint is to

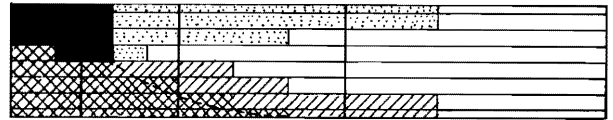


Figure 6. Effect of Support Restraint on Damage Zone. ($\rho = 3.14\%$; $P_u = 112.5$ kN; Shading as in Figure 5).

reduce the zone of cracking damage (by virtue of in-plane compressive forces) and allow a greater percentage of the true punching capacity to be mobilized. A restrained slab with a given percentage of steel behaves as an unrestrained slab of increased ρ . It thus followed that the beneficial effect of edge restraint on the collapse load will taper off with increase in main reinforcement percentage, as the two effects basically act in the same way to enhance the capacity, leading to redundancy. This finding corroborates the experimental evidence of several research groups [1–4].

4.1.2. Influence of Shear Degradation

The cracked concrete is modeled to lose shear stiffness gradually as the cracks become wider, where according to [17], the cracked shear modulus G^c may be taken as

$$G^c = 0.25 G(1 - \epsilon/\epsilon_c) \quad (14)$$

with $G^c = 0$ if the strain across the crack ϵ exceeds the fictitious strain ϵ_c . Results of numerical experiments on shear critical RC beams indicated ϵ_c to be in the neighborhood of 0.004 to 0.005.

In order to see the influence of shear degradation, slabs with two different percentages of steel were analyzed, for three different cases:

1. No degradation *i.e.* $G^c = G$
2. Normal degradation (as per Equation (14), $\epsilon_c = 0.005$)
3. Full degradation (*i.e.* $G^c \approx 0$ on first cracking).

Results for the various cases are indicated in Table 1. The percent difference between full degra-

Table 1. Influence of Shear Degradation on Failure Load.

Total Reinforcement ρ	Failure Load (kN)			% Difference (2)–(4)/(4)
	(1)	(2)	(3)	
3.14%	113	99	94.5	19.5
1.57%	94.5	81.3	73	29.5

dation and no degradation is higher for the case of lower total reinforcement ($\rho = 1.57\%$), which shows that the collapse load is more sensitive to shear transfer modeling across cracks where cracked zones form a greater component of the potential collapse surface.

4.2. Implications for Girder–Slab Deck Systems

The results of the previous section have revealed the close interaction between the amount of main reinforcement and the true punching shear collapse mode, which is the highest capacity that the slab can attain prior to the localized failure. In the case of girder–slab bridge deck systems where the slab itself is not too thick, and total slab reinforcement in the two directions is of the order of $\rho = 2\%$, the problem of reduced collapse load by virtue of crack propagation under repetitive loading becomes real.

In order to simulate this effect, a numerical experiment was carried out. The experiment was conducted on the same panel as used in the previous section with initial total $\rho = 1.57\%$. It was patch loaded to 54% of its collapse load, using a central $101.6 \text{ mm} \times 101.6 \text{ mm}$ ($4 \text{ in} \times 4 \text{ in}$) patch. The damage zone was recorded (Figure 7) and the slab unloaded. The steel reinforcement was now increased to total $\rho = 6.28\%$, and the damaged slab was reloaded to failure. Failure of this slab occurred at 66% of its virgin strength recorded earlier as 129.5 kN. The reason for this reduction is that the cracking damage zone at the initial loading stage exceeded the cracking damage near ultimate conditions of a corresponding healthy panel ($\rho = 6.28\%$) loaded monotonically to failure. Thus the full punching capacity of the damaged slab could not be mobilized due to presence of extended separation zones over the potential collapse surface.

The foregoing experiment illustrates vividly that the propagation of cracks under repeated loadings of a bridge deck will reduce the collapse load associated with a localized failure. The localized failure of a slab reinforced only with main reinforcement is crack or notch sensitive, and is of unstable type as opposed to a pure flexural failure which is normally stable. The latter requires increasing loads to extend cracking zones further, whereas the shear–flexure mode of failure in the absence of shear reinforcement is unstable, and highly effected by extent of tension cracking damage zones.

The philosophy of using minimal main reinforcement in deck slabs [12] should be reconsidered,



Figure 7. Damage Zone at $P/P_u = 0.54 \text{ kN}$. ($\rho = 1.57\%$; Shading as in Figure 5).

especially in areas where repeated loads of high magnitude are known to occur. Experience has shown that under heavy service loads, the probable mode of failure in a girder–slab or box girder deck system is the localized “pot hole” type of failure [20]. In the absence of shear reinforcement, sufficient amount of main reinforcement for a given slab thickness should be provided in order to minimize intrusion of two way cracking damage and preclude premature localized failure.

5. CONCLUSIONS

A nonlinear finite element model with components embedded to simulate damage due to tension cracking, shear-compression yielding and crushing of concrete and elasto-plastic response of reinforcement is seen to simulate realistically the transformation of failure modes resulting due to variation in steel percentage ρ , and also to exhibit enhancement in collapse load of laterally restrained slabs.

The definition of true punching capacity under central patch loads of small size is enunciated as the phenomenon dominated by plastic yielding of concrete with minimal tension cracking damage, and is shown to be approached asymptotically with increasing percentage of main steel reinforcement.

On the other end of the spectrum, at very low levels of main reinforcement, failure is seen to be dominated by two way tension cracking and reinforcement yielding and constitutes the classical flexural failure. For low to medium levels of reinforcement, the failure modes exhibit damage components defined as a flexure–shear interactive failure.

In order to minimize the most probable mode of failure in thin slabs of girder–slab or box girder deck systems under repeated cycles of heavy service loads, an amount of main reinforcement close to maximum permissible should be provided to pre-empt localized pot hole types of failure. This philosophy would help in upgrading bridge deck slabs which may be considered adequate for conditions at time of design to meet increased loading requirements of the future.

NOTATION

E_c	= modulus of elasticity of concrete
E_s, E'_s	= elastic and tangent moduli of steel, respectively
f'_c	= concrete compressive strength
f_t	= concrete tensile strength
f_y	= steel yield strength
ϕ	= angle of internal friction
θ	= angle of similarity
$d\lambda$	= proportionality constant for plastic vector
$\sigma_x, \sigma_y, \sigma_z$	= deviatoric normal stresses in x , y , and z directions
ϵ_u	= crushing strain of concrete
ϵ_c	= fictitious cracking strain used to downgrade shear modulus G
ϵ_m, α	= tension stiffening parameters.

ACKNOWLEDGEMENT

The authors wish to acknowledge the considerable computer support extended by King Fahd University of Petroleum & Minerals in the execution of this work. They are also grateful to Mr. Solano P. Cruz for typing this manuscript.

REFERENCES

- [1] R. Taylor and B. Hayes, "Some Tests on the Effect of Edge Restraint on Punching Shear in Reinforced Concrete Slabs", *Magazine of Concrete Research*, **1.17(50)** (1965), p. 39.
- [2] P. Y. Tong and B. deV. Batchelor, "Compressive Membrane Enhancement in Two-Way Bridge Slabs", *Cracking, Deflection and Ultimate Load of Concrete Slab Systems*, American Concrete Institute Publication, SP-30, 1971, p. 271.
- [3] ASCE-ACI Committee 426, "The Shear Strength of Reinforced Concrete Members—Slabs", *Journal of the Structural Division, ASCE*, **100(ST8)**, Proc. Paper 10733, (1974), p. 1543.
- [4] Y. Aoki and H. Seki, "Shearing Strength and Flexural Cracking and Capacity of Two-Way Slabs Subjected to Concentrated Load", *Cracking, Deflection and Ultimate Load of Concrete Slab Systems*, American Concrete Institute Publication, SP-30, 1974, p. 103.
- [5] P. E. Regan, "The Dependence of Punching Resistance upon the Geometry of the Failure Surface", *Magazine of Concrete Research*, **36(126)** (1984), p. 3.
- [6] P. E. Regan, "Symmetric Punching of Reinforced Concrete Slabs", *Magazine of Concrete Research*, **38(136)** (1986), p. 115.

- [7] I. A. E. M. Shehata and P. E. Regan, "Punching in R.C. Slabs", *Journal of the Structural Division, ASCE*, **115(7)** (1989), p. 1726.
- [8] S. Kinnunen and H. Nylander, "Punching of Concrete Slabs Without Shear Reinforcement", *Transactions of the Royal Institute of Technology, Stockholm, Sweden*, No. 158, 1960.
- [9] J. F. Brotchie and M. H. Holley, "Membrane Action in Slabs", *ACI SP-30*, 1971, p. 345.
- [10] J. R. Eyre and K. O. Kemp, "A Graphical Solution for Predicting the Increase in Strength of Concrete Slabs", *Magazine of Concrete Research*, **35(124)** (1983), p. 151.
- [11] P. F. Csagoly, "Design of Thin Concrete Deck Slabs by the Ontario Highway Bridge Design", *Report SRR79-11, Ministry of Transportation and Communications, Canada*, May 1979.
- [12] *Ontario Highway Bridge Design Code, 2nd Edn.* Ministry of Transportation and Communications, Highway Engineering Division, Ontario, Canada, 1983.
- [13] M. W. Braestrup, M. P. Nielson, B. C. Jensen, and F. Bach, "Axisymmetric Punching of Plain and Reinforced Concrete", *Lyngby, Technical University of Denmark, Structural Research Laboratory, Report No. R75*, 1976, p. 33.
- [14] M. W. Braestrup and C. T. Morley, "Dome Effect in RC Slabs: Elastic-Plastic Analysis", *Journal of the Structural Division, ASCE*, **106(ST6)** (1980), p. 1255.
- [15] D. H. Jiang and J. H. Shen, "Strength of Concrete Slabs in Punching Shear", *Journal of the Structural Division, ASCE*, **112(12)** (1986), p. 2578.
- [16] D. R. J. Owen and J. A. Figueiras, "Ultimate Load Analysis of Reinforced Concrete Plates and Shells Including Geometric Nonlinear Effects", in *Finite Element Software for Plates and Shells*. eds. E. Hinton and D. R. J. Owen. Swansea, U.K.: Pineridge Press, 1984, p. 327.
- [17] L. Cedolin and S. D. Poli, "Finite Element Studies of Shear-Critical R/C Beams", *Journal of Engineering Mechanics Division, ASCE*, **103(EM3)** (1977), p. 395.
- [18] D. R. J. Owen and E. Hinton, *Finite Elements in Plasticity—Theory and Practice*. Swansea, U.K.: Pineridge Press, 1980.
- [19] K. Kareem, "Load Induced Cracking and Failure of Concrete Deck Slabs in Girder-Slab Type Bridges", *M.S. Thesis, Department of Civil Engineering, King Fahd University of Petroleum & Minerals, Dhahran, Saudi Arabia*, January 1989.
- [20] M. Y. Al-Mandil, A. K. Azad, M. H. Baluch, D. Pearson-Kirk, and A. M. Sharif, "A Study of Cracking of Concrete Bridge Decks in Saudi Arabia", *vol. I-III. King Abdulaziz City for Science and Technology, Riyadh, Saudi Arabia*, June 1989.

Paper Received 21 November 1990; Revised 11 May 1991.